Selectively Improving the Bio-Oil Quality by Catalytic Fast Pyrolysis of Heavy-Metal-Polluted Biomass: Take Copper (Cu) as an Example

6 AUTHORS, INCLUDING:

Hong Jiang
University of Science and Technology of China
55 PUBLICATIONS **641** CITATIONS

Xuesong Zhang
University of Science and Technology of China
12 PUBLICATIONS **180** CITATIONS

Han-Qing Yu
University of Science and Technology of China
**508** PUBLICATIONS **11,036** CITATIONS

Selectively Improving the Bio-Oil Quality by Catalytic Fast Pyrolysis of Heavy-Metal-Polluted Biomass: Take Copper (Cu) as an Example

Wu-Jun Liu, Ke Tian, Hong Jiang,* Xue-Song Zhang, Hong-Sheng Ding, and Han-Qing Yu

Department of Chemistry, University of Science and Technology of China, Hefei 230026, China

Ⓢ Supporting Information

ABSTRACT: Heavy-metal-polluted biomass derived from phytoremediation or biosorption is widespread and difficult to be disposed of. In this work, simultaneous conversion of the waste woody biomass into bio-oil and recovery of Cu in a fast pyrolysis reactor were investigated. The results show that Cu can effectively catalyze the thermo-decomposition of biomass. Both the yield and high heating value (HHV) of the Cu-polluted fir sawdust biomass (Cu-FSD) derived bio-oil are significantly improved compared with those of the fir sawdust (FSD) derived bio-oil. The results of UV–vis and ^1H NMR spectra of bio-oil indicate pyrolytic lignin is further decomposed into small-molecular aromatic compounds by the catalysis of Cu, which is in agreement with the GC-MS results that the fractions of C7–C10 compounds in the bio-oil significantly increase. Inductively coupled plasma-atomic emission spectrometry, X-ray diffraction, and X-ray photoelectron spectroscopy analyses of the migration and transformation of Cu in the fast pyrolysis process show that more than 91% of the total Cu in the Cu-FSD is enriched in the char in the form of zerovalent Cu with a face-centered cubic crystalline phase. This study gives insight into catalytic fast pyrolysis of heavy metals, and demonstrates the technical feasibility of an eco-friendly process for disposal of heavy-metal-polluted biomass.
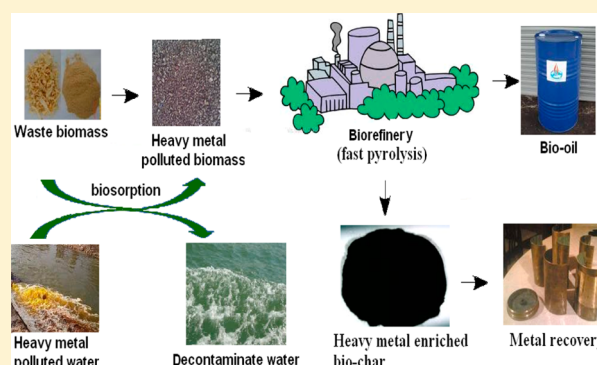
INTRODUCTION

The increasing heavy metal pollution of surface and ground waters, with largely unknown long-term effects on wildlife and human health, can easily lead to serious environmental problems.[1,2] The total anthropogenic inputs of heavy metals (e.g., Zn, Cr, Ni, Pb, Cu, Cd, and Hg) to aquatic systems were about $0.3-1.0 \times 10^6$ tons annually.[3,4] A lot of effort has been expended on developing techniques to effectively remove the heavy metals.[5–7] Among these, phytoremediation and biosorption are two promising low-cost technologies for treating heavy-metal-polluted wastewater.[8–11] Phytoremediation is widely used in the remediation of heavy-metal-polluted water bodies or soils with low heavy metal concentration, whereas biosorption with lifeless waste biomass is suitable for the industrial effluent containing high concentration of heavy metals.

Unfortunately, in both the phytoremediation and biosorption processes, after metal accumulation, the used biomass is polluted by heavy metals and difficult to be disposed of. To process the polluted biomass in an environmentally friendly manner is a key problem limiting the widely use of phytoremediation and biosorption. A common method for treating this type of biomass is to desorb heavy metals by using strong inorganic acid or EDTA solutions, which can recover over 95% of the adsorbed metals.[12,13] However, many inherent disadvantages limit its wide application. For example, a huge volume of solution is needed in the leaching process (often more than 20 mL of leaching solution to 1 g of spent biomass), and the discharge of the spent leaching solution or deposit of the leached biomass increases the treatment expenditure and causes secondary pollution.

Alternatively, fast pyrolysis is a preferable technology for converting heavy-metal-polluted biomass (HMPB) into bio-oil, which can be used as fuel or chemical feedstock.[14–16] Unlike direct combustion for the HMPB disposal under aerobic conditions, which may produce many toxic pollutants,[17] for example, polycyclic aromatic hydrocarbons and dioxins, the fast pyrolysis is completed under anaerobic conditions, and the emission of such pollutants can be avoided. In our previous work, the techno-economic feasibility of fast pyrolysis of the HMPB in laboratory scale has been demonstrated.[18] In the pyrolysis process, heavy metals are mainly enriched in residual pyrolysis char, while both bio-oil and noncondensable fractions contain a very low amount of heavy metals. These findings suggest that the pyrolysis of HMPB is an environmentally friendly process, and that the produced bio-oil can find its applications in many fields without secondary pollution of heavy metals.

In contrast, many heavy metals usually exhibit a high catalytic activity in many chemical reactions and have been extensively used as catalysts in organic synthesis, pollutant degradation, and catalytic reforming.[19−24] The heavy-metal-containing catalysts are also widely used in the catalytic thermochemical conversion of biomass into high-quality fuels or value-added chemicals, and usually show a favorable catalytic activity or selectivity.[25−27] However, preparing such metal catalysts which involves multifarious physical and/or chemical treatments and employing them in biomass pyrolysis process are costly and time-consuming.[28−30] Therefore, taking full advantage of the catalytic roles of the heavy metals inherent in HMPB in the pyrolysis process to improve product quality is a promising attempt in the comprehensive utilization of HMPB. Moreover, increasing the selectivity of thermal decomposition of waste biomass has attracted interest in recent years. As far as we know, little information is available about in situ catalytic effect of heavy metals on the HMPB pyrolysis and the transformation of heavy metals in fast pyrolysis process.

Herein, copper (Cu), a typical heavy metal, which is often present in industrial effluents or even natural waters, was selected as a target heavy metal, while fir sawdust (FSD), an abundantly available lignocellulosic waste biomass, was used as the model biomass. The main objectives of this work are (1) to investigate the catalytic effect of Cu on the fast pyrolysis of Cu-polluted fir sawdust (Cu-FSD); and (2) to explore the migration and transformation of Cu in fast pyrolysis process. For this purpose, the effects of main operating parameters, including pyrolysis temperature and Cu content, were investigated. The UV−vis spectrophotometer, ^{1}H NMR, and GC-MS were used to analyze the bio-oil, and the catalytic selectivity of Cu on bio-oil was explored. The distribution and chemical speciation of Cu in different pyrolysis products, that is, bio-oil and char, were characterized by X-ray photoelectron spectroscopy (XPS) and X-ray diffraction (XRD). This study provides a new approach for recycling energy and resource as well as eliminating the heavy metal pollution.

■ EXPERIMENTAL SECTION

Materials. The FSD biomass was obtained from a local timber treatment plant in Hefei, China. The biomass was first washed several times with distilled water to remove the dust particles and then dried in an oven at 378 K until the constant moisture was reached. The dried biomass was crushed by a high-speed rotary cutting mill and the produced particles with the size smaller than 0.12 mm (120 mesh) were collected and stored for further use. The proximate and ultimate analysis results of the FSD are shown in Table S1 (Supporting Information (SI)). Analytical grade CuSO$_4$, purchased from Sinopharm Chemical Reagent Co., Ltd. China, was used as Cu source.

The Cu-FSD was prepared in a biosorption process using FSD as an adsorbent, and the adsorption experiments were carried out in a series of 250 mL conical flasks at 298 K. A certain amount of FSD and 100 mL of Cu^{2+} solution at different concentrations were mixed in the flasks and shaken in a constant-temperature oscillator at 200 rpm. After the adsorption was accomplished with reaction time of 300 min, the mixture was dried at 378 K and then sieved again to collect the particles with a size smaller than 0.12 mm for further use.

Fast Pyrolysis of Cu-FSD. The fast pyrolysis experiments were carried out in a vertical drop fixed bed reactor described in SI (Figure S1).[31] A 5 g portion of Cu-FSD sample was placed in the feed pipe at the beginning of the pyrolysis. Soon after the temperature reached the setting value (723−873 K), a nitrogen flow of 400 mL min^{-1} was supplied and maintained for 20 min to remove air from the pyrolysis system. Thereafter, the Cu-FSD sample was fed into the quartz tubular reactor via a piston. The temperature of the biomass increased from room temperature to the reactor temperature in its falling process within about 1−2 s at a heating rate over 300 K/second. The volatiles produced in the pyrolysis process were swept out by nitrogen gas at a flow rate of 200 mL min^{-1}. The condensable components in volatiles were condensed by a cold ethanol−ethylene glycol mixture (1:1, v/v) to produce bio-oil. When the pyrolysis process was completed, the quartz tubular reactor was immediately moved out from the heating zone and the char was cooled to room temperature in a nitrogen gas flow of 200 mL min^{-1}. The produced char and bio-oil were weighted to determine their yields and stored in a refrigerator for further analysis and gas yields were determined by difference. Each pyrolysis experiment was conducted twice and the results were given in average values.

Analysis. The hydrogen (H), carbon (C) and nitrogen (N) contents in the bio-oil and char were determined using an elemental analyzer (VARIO EL III, Elementar Inc., Germany), while their oxygen (O) contents were calculated by difference. The thermal stability of the FSD was characterized with a DTG-60H/DSC-60 thermogravimetric analyzer (Shimadzu Co., Japan) and the result is shown in SI Figure S4.

To determine Cu contents in the Cu-FSD, char and bio-oil samples, a preliminary digestion was performed with concentrated sulfuric acid in an oil-bath at 473 K, and then with hydrogen peroxide (30%, v/v) until the digested solution became transparent. Then, the volume of digested solution was made up to 100 mL using deionized water. The Cu concentration in the digested solution was determined by inductively coupled plasma-atomic emission spectrometry (ICP-AES, Optima 7300 DV, Perkin-Elmer Co., Waltham, MA) and the Cu contents in the Cu-FSD, char and bio-oil samples were calculated correspondingly.

XPS was used to analyze the compositions and valence state changes of Cu in the pyrolysis process. The XPS spectra of Cu-FSD and the pyrolysis char were obtained with an X-ray photoelectron spectrometer (ESCALAB250, Thermo-VG Scientific Inc., UK) using monochromatized Al Kα radiation (1486.92 eV). XRD analysis of the Cu-FSD and pyrolysis char samples was carried out in an 18-KW rotating anode X-ray diffractometer (MXPAHF, Japanese Make Co., Japan) utilizing nickel-filtered Cu Kα radiation source (30 kV/160 mA, λ = 1.54056 Å). The samples were scanned from 20° to 80° at a scan rate (2θ) of 0.02°/s.

The UV-vis spectra of the bio-oil were recorded on a UV-vis spectrophotometer (UV-1700, Phenix Co., Ltd. China). Before analysis, the samples were prepared by dissolving accurately weighed ∼50 mg of bio-oil in anhydrous ethanol and making the volume up to 50 mL. Spectra were acquired at wavelength scanning from 200 to 600 nm.

The ^{1}H NMR spectra of the bio-oil were recorded with a 400 MHz nuclear magnetic resonance spectrometer (AV 400, Bruker Inc., Switzerland) at room temperature. The NMR experiments were quantitative, and the samples were prepared by dissolving accurately weighed ∼50 mg of bio-oil in acetone-d$_6$. In spectra analysis, the integration values of given peaks were compared to the total area of all peaks, resulting in mol.% units.

Before the GC-MS analysis, the bio-oil samples were separated into two fractions through dichloromethane (CH_2Cl_2) extraction. The compounds in the CH_2Cl_2 soluble fraction were analyzed by gas chromatography−mass spectrometry (GC-MS, 7890A GC/5975C MS with a HP-5MS nonpolar capillary column, 30 m × 0.25 mm × 0.25 μm, Agilent Inc., Santa Clara, CA). High purity helium gas was employed as carrier gas at a constant flow rate of 1.0 mL min^{-1}, and a split of the carrier gas (1:20) was used. The temperature of the GC-MS injector was 523 K. The GC oven temperature was programmed from 313 to 453 at 4 K min^{-1} and then to 523 at 10 K min^{-1}, and the final temperature was kept for 5 min.

■ RESULTS AND DISCUSSION

Pyrolysis Performance of the Cu-FSD and FSD. Temperature is a key factor influencing the yields and compositions of pyrolytic products, i.e., bio-oil, char, and gas.[32,33] The distributions of the pyrolytic products of FSD and Cu-FSD in Figure 1 show that the char yields in both FSD and
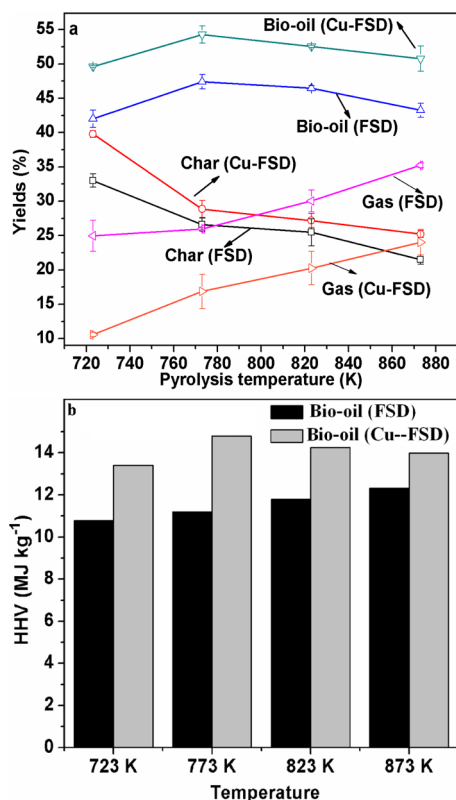

Figure 1. (a) Yields of the pyrolytic products such as bio-oil, char and gas at different temperatures (Cu content in the Cu-FSD was 1.09 wt %, %, daf); (b) HHVs of the bio-oil obtained at different pyrolysis temperatures. The HHV was calculated with the following formula HHV (MJ/kg) = (3.55 C^2−232 C − 2230 H+51.2 C × H+131 N +20600)/1000. [37].

Cu-FSD pyrolysis monotonously decreased with the increasing temperature, while the gas yields increased with an increase in temperature. This result is consistent with those reported in literature.[34,35]

At a low temperature, the volatile matter of the biomass cannot be completely pyrolyzed to produce bio-oil. While at a high temperature, the pyrolytic vapor might crack partially into incondensable gas, both leading to a reduced bio-oil yield.[36]

Thus, there should be an optimum temperature for the maximum bio-oil yield in the fast pyrolysis process. Figure 1a shows a maximum yield of bio-oil for both FSD and Cu-FSD at 773 K, which is in agreement with the analysis above. The bio-oil yields of the Cu-FSD pyrolysis were higher than those of the FSD pyrolysis at all temperatures. This can be attributed to the catalytic effect of Cu on the pyrolysis process. The presence of Cu also decreased the oxygen content in bio-oils (SI Table S2), and thus significantly increased the high heating value (HHV) of the bio-oil. As shown in Figure 1b, the HHVs of the FSD derived bio-oils were in a range of 10.77−12.32 MJ kg^{-1}, while those of the Cu-FSD derived bio-oil ranged from 13.42 to 14.79 MJ kg^{-1}, which was about 23% higher than those of the FSD derived bio-oil. This result suggests that Cu in the Cu-FSD shows a catalytic effect on the improvement of the bio-oil property for fuel application.

A series of fast pyrolysis experiments were carried out by changing the Cu contents of the Cu-FSD at 773 K. Figure 2a
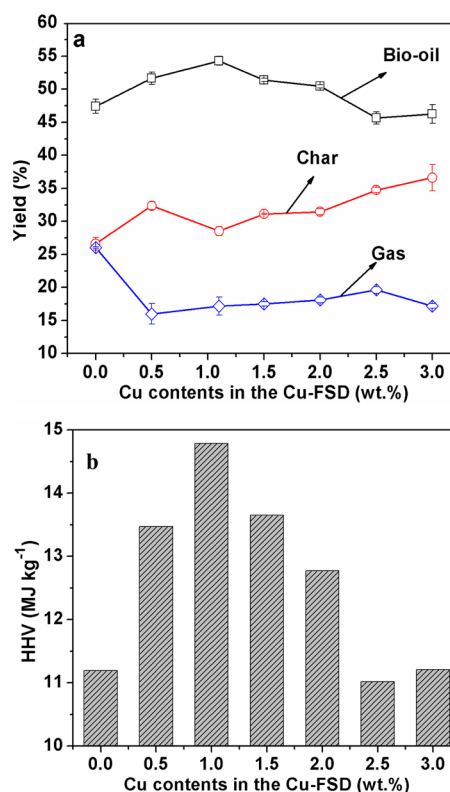

Figure 2. (a) Yields of the products in the pyrolysis of the Cu-FSD with different Cu contents, %, daf; (b) HHVs of the bio-oil obtained in the pyrolysis of the Cu-FSD with different Cu contents (The pyrolysis temperature here was fixed at 773 K).

illustrates the product yields versus Cu contents in the fast pyrolysis of Cu-FSD. The char yields of Cu-FSD were higher than those of FSD (0 wt % of Cu content), and slightly increased with the increasing Cu contents, except for 0.5 wt %; while the gas yields of Cu-FSD were significantly lower than those of FSD and were almost unaffected by the Cu contents. The lower gas yield for the biomass pyrolysis with Cu might be attributed to the further reactions of the gas composition, for example, H_2, light hydrocarbons (C_xH_y), with the bio-oil or biochar species catalyzed by Cu. For example, Cu is able to catalyze the reaction between H_2 with pyrolytic lignin to form some phenolic compounds.[38] The presence of Cu may also

C

dx.doi.org/10.1021/es204681y | Environ. Sci. Technol. XXXX, XXX, XXX−XXX

promote the aromatization of C_xH_y in gas phase to form more aromatic compounds and condense in bio-oil phase, thus decreasing the gas yield.[39]

The bio-oil yields increased from 47.4% to 54.3% with a Cu content increase from 0 to 1.0 wt % with a maximum value at 1.0 wt % of Cu content. With a further increase in Cu content until 2.5 wt %, the bio-oil yields continuously decreased, and then keep almost unchanged, which were lower than that of FSD (47.4%). This tendency was similar to that of pyrolysis of corncob catalyzed by fluidized catalytic cracking catalysts.[40] The HHVs of the bio-oil show the same trend as the bio-oil yields. The maximum HHV of the bio-oil appeared at Cu content of 1.0 wt % (14.79 MJ kg^{-1}), while the values at Cu contents of 2.5 and 3.0 wt % sharply decreased to 11.02 and 11.21 MJ kg^{-1}, respectively, even lower than those of the FSD derived bio-oil. Therefore, the optimum Cu content with the most favorable catalytic effect on the Cu-FSD pyrolysis was 1.0 wt %, at which the produced bio-oil had the greatest yield and HHV. This phenomenon can be explained as follows: the presence of Cu in a catalytic amount,for example, <1 wt %, could promote the deoxygenation reactions,[41] thus decrease the oxygen contents of the bio-oil and increase the HHV of the bio-oil. However, when Cu content in biomass was further increased, the catalytic deoxygenation effect of Cu was exceeded by its oxidation effect, because Cu(II) acted as an oxidant (Cu(II) +2 e$^-$ = Cu(0), E$_0$ = 0.34 V),[42] resulting in an increased oxygen contents and decreased HHV of the bio-oil.

Bio-Oil Analysis. The UV−vis spectra of the FSD and Cu-FSD derived bio-oils are shown in Figure 3. The two
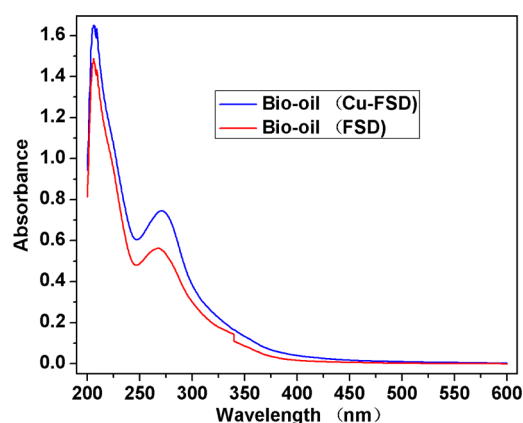

Figure 3. The UV-vis spectra of the FSD and Cu-FSD derived bio-oil.

absorption peaks at 206 and 270 nm are attributed to the characteristic E2 and B absorption bands of aromatic ring,

respectively. Comparing the spectra of the FSD and Cu-FSD derived bio-oils indicates that there is no difference among peak positions, but the peak intensities are significantly different. The peak intensities of Cu-FSD derived bio-oil are 1.65 (E2 band) and 0.75 (B band), higher than those of FSD derived bio-oil (1.49 and 0.56 for E2 and B band, respectively), indicating that the content of aromatic components in the Cu-FSD derived bio-oil is much higher than that in FSD derived bio-oil.

The ^{1}H NMR spectra were used to analyze the compositions of bio-oil based on the chemical shift of H atoms in different chemical environment (the NMR spectra of FSD and Cu-FSD derived bio-oils are presented in SI Figure S2). The results in Table 1 show that contents of H atoms attached in all functional groups (i.e., aliphatic, methoxyl, hydroxyl, aromatic, and aldehyde) of the Cu-FSD derived bio-oil have a significant increase compared to those of FSD derived bio-oil. For example, the H in aromatic groups of Cu-FSD derived bio-oil is 6.84 mol.%, almost twice of that in the FSD derived bio-oil (3.47 mol.%). The aromatic compounds in the bio-oil are derived mainly from the lignin structure, one of the key biomass building blocks.[38,43] Therefore, the increase in aromatic compounds suggests that the presence of Cu (∼1 wt.%) can promote the thermal decomposition of the lignin structure into small-molecular aromatic compounds.

The GC−MS was used to analyze the volatile components of bio-oils (extracted by CH_2Cl_2), and the identified compounds are listed in Table 2. The bio-oil of both derivations was a complex mixture which contained a wide variety of oxygenated organic compounds, for example, carboxylic acids, ketones, alcohols, ethers, and phenols. This is analogous with the bio-oil from other sources.[44,45] The compound compositions of the Cu-FSD derived bio-oil were similar with those of the FSD derived bio-oil, except that five new compounds were found in the Cu-FSD derived bio-oil and four compounds were not found.

The contents of the organic compounds in the Cu-FSD and FSD derived bio-oils changed significantly. Most of the compounds in the bio-oil contained two or more functional groups and it is difficult to exactly classify them according to their functional groups. Therefore, in this study, the organic compounds in the bio-oil were classified by the amount of carbon atoms (e.g., C3 represents all the compounds whose molecules contain three carbon atoms), and the distribution of compounds with different carbon atom amounts is illustrated in Figure 4. C7−C10 compounds, regarded as completely chain-breaking decomposed products of lignin in biomass,[38] were the main categories in the bio-oils of both derivations, which occupied a large proportion in both bio-oils, that is, 66.5% for the FSD derived bio-oil and 80.9% for the Cu-FSD derived bio-

Table 1. ^{1}H NMR Chemical Shift Assignment Ranges and Functional Group Attributions for the FSD and Cu-FSD Derived Bio-Oils (^{a}Based on the H atoms contents)
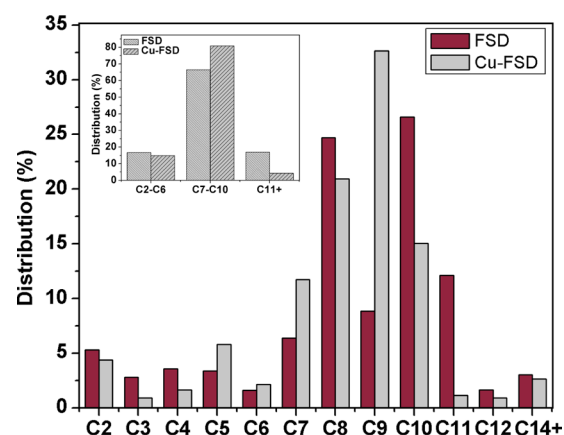
chemical shift range (ppm)	functional group attributions	functional group contents (mol. %)^a	
		FSD	Cu-FSD
0.5-3.0	aliphatic (**H**-C-R)	37.62	41.46
3.0-3.4	methoxyl (**H**$_3$C-O-R)	3.70	3.91
3.4-3.7	water (**H**$_2$O)	48.01	37.34
3.7-5.5	hydroxyl (**H**-O-R)	6.07	8.51
6.0-8.2	aromatic (**H**-◯-R)	3.47	6.84
9.2-10.0	aldehyde (**H**C(=O)-R)	0.10	1.19

Table 2. Relative Proportions (Area %) of the Compounds of the FSD and Cu-FSD (Cu Content: 1.09 wt %) Derived Bio-Oil[a]

R. T. (min)	molecular formula	compounds assignment	% area	
			FSD	Cu-FSD
2.27	$C_2H_4O_2$	acetic acid	5.31	4.39
2.41	$C_4H_8O_2$	3-hydroxylbutanal	3.30	1.29
2.54	$C_3H_6O_2$	1-hydroxypropan-2-one	2.79	0.72
3.98	$C_5H_{10}O_2$	1-hydroxyl-3-methybutan-2-one	0.16	0.23
4.59	$C_4H_6O_3$	4-methyl-1,3-dioxolan-2-one	0.29	0.37
4.93	$C_3H_4O_3$	1,3-dioxolan-2-one	ND	0.18
5.04	$C_5H_{10}O_2$	cyclopentane-1,3-diol	1.14	1.02
6.58	$C_7H_{12}O_2$	3,4,4-trimethyldihydrofuran-2(3H)-one	0.80	ND
6.78	C_5H_6O	cyclopent-2-enone	0.98	1.03
7.03	$C_5H_4O_2$	furan-2-carbaldehyde	ND	3.28
8.60	$C_6H_{10}O_2$	3-methylpentane-2,4,-dione	0.28	0.19
9.76	C_6H_8O	2,4-dimethylfuran	0.45	0.13
11.03	$C_5H_6O_2$	2-hydroxylcyclopent-2-enone	0.40	0.23
14.06	$C_8H_{12}O_3$	2-hydroxy-6-methycyclohex-3-enecarboxylic acid	ND	0.17
15.24	$C_5H_8O_3$	2,3-dihydroxycyclopentanone	0.69	ND
15.34	$C_6H_8O_2$	3-methylcyclopentane-1,2-dione	0.34	0.12
17.41	$C_7H_8O_2$	4-methoxyphenol	5.57	11.23
21.27	$C_8H_{10}O_2$	2-methoxy-4-methylphenol	15.16	12.03
22.29	$C_6H_{12}O_2$	3-methylcyclopentane-1,2-diol	ND	0.89
24.31	$C_9H_{12}O_2$	4-ethyl-2-methoxyphenol	3.05	19.69
25.57	$C_9H_{10}O_2$	1-(2-hydroxy-5-methylphenyl)ethanone	5.79	12.95
26.95	$C_8H_{10}O_3$	2,6-dimethoxyphenol	8.69	5.24
27.21	$C_6H_6O_3$	benzene-1,2,4-triol	0.53	0.82
28.60	$C_{10}H_{12}O_2$	2-methoxy-4-(prop-1-en-1-yl)phenol	19.30	6.20
29.21	$C_{10}H_{10}O_4$	4-formyl-2-methoxyphenyl acatate	0.25	8.75
31.82	$C_{14}H_{22}O$	2,4-ditert-butylphenol	ND	0.95
32.23	$C_{12}H_{19}O_3N$	1-(2,3,5-trimethoxyphenyl)propan-2-amine	1.64	0.92
33.42	$C_{10}H_{12}O_3$	1-(2,4-dimethoxyphenyl)ethanone	6.62	0.11
34.27	$C_{10}H_{14}O_2$	2-hydro-4-methoxy-3,6-dimethylbezaldehyde	0.43	ND
34.45	$C_{11}H_{14}O_3$	4-allyl-2,6-dimethoxylphenol	10.06	0.18
35.87	$C_{11}H_{14}O_3$	4-ethyl-2,5-dimethoxylbenzaldehyde	0.61	ND
36.16	$C_7H_6O_4$	2,4-dihydroxybenzoic acid	ND	0.51
39.27	$C_{11}H_{14}O_4$	1-(2,6-dihydroxy-4-methoxyphenyl)butan-1-one	1.46	0.97
40.32	$C_{15}H_{14}O_3$	benzyl 2-methoxybenzoate	0.51	0.53
43.18	$C_8H_8O_5$	2-(3,4-dihydroxyphenyl)-2-hydroxyacetic acid	0.86	4.17
43.72	$C_{17}H_{18}O_4$	2-(4-(benzyloxy)-3-ethoxyphenyl) acetic acid	2.53	0.50

[a]ND means not detected.

Figure 4. Distribution of the compounds in the FSD and Cu-FSD derived bio-oils, and distribution of C2−C6, C7−C10, and C11+ compounds in the bio-oils (the inset figure).

Behavior of Cu in the Pyrolysis. The Cu distribution in the char (Cu(char)%) and in the bio-oil (Cu(bio-oil)%) are calculated by eqs 1 and 2

$$Cu(char)\% = \frac{(Cu\ contents\ in\ the\ char) \times (weight\ of\ the\ produced\ char)}{(Cu\ contents\ in\ the\ Cu\text{-}FSD) \times (weight\ of\ Cu\text{-}FSD)} \times 100\% \quad (1)$$

$$Cu(bio\text{-}oil)\% = \frac{(Cu\ contents\ in\ the\ bio\text{-}oil) \times (weight\ of\ the\ the\ bio\text{-}oil)}{(Cu\ contents\ in\ the\ Cu\text{-}FSD) \times (weight\ of\ Cu\text{-}FSD)} \times 100\% \quad (2)$$

The Cu(char)% and Cu(bio-oil)% of the Cu-FSD (Cu content of 1.09% in wt) pyrolysis at different temperatures are shown in Figure 5a. The Cu(bio-oil)% increased with the elevation of temperature, whereas the Cu(char) presented a reverse trend with the temperature. Due to the poor volatility of Cu, it mainly retained in the char with more than 90%. This result is similar to the report of Stals et al.[46] The Cu contents in the char ranged from 2.6 to 3.9 wt % (SI Table S4), much higher than those in the Cu-FSD. After burning in the fast pyrolysis system, the Cu contents in the remained char-ash was concentrated by over 30 wt.%, and the Cu recovery was 98.9% when the biochar was combusted at 873 K for 4 h. With an increase in combustion temperature to 1173 K, the Cu recovery only slightly decreased to 94.5% (Figure 5b), indicating that there was no significant volatilization of Cu during the combustion. In the bio-oil, the Cu content was only 4.6−7.6 mg kg^{−1} (SI Table S4). This implies that, when used as a fuel, such a bio-oil brings about negligible heavy metal pollution.

Transformation of Cu in the Fast Pyrolysis Process. Fast pyrolysis is a very complex process and involves various chemical reactions.[47] In such a process, the existing form and chemical state of Cu in the Cu-FSD changed significantly, as evidenced by the XRD results (Figure 6). The XRD profiles of the Cu-FSD and char show that the diffraction peak of Cu-FSD at $2\theta = 22.9°$, which is attributed to the lignocellulose (002) crystal plane, disappeared after pyrolysis. This confirms the decomposition of liginocellulose structure in the pyrolysis process. The diffraction peaks of the char at $2\theta = 43.5°$, 50.7° and 74.2° are deemed to the Cu (111), (200), and (210) crystal plane, respectively, indicating that the Cu present in the char was in metallic form with a face-centered cubic crystal (JCPDS file: 04-0836).
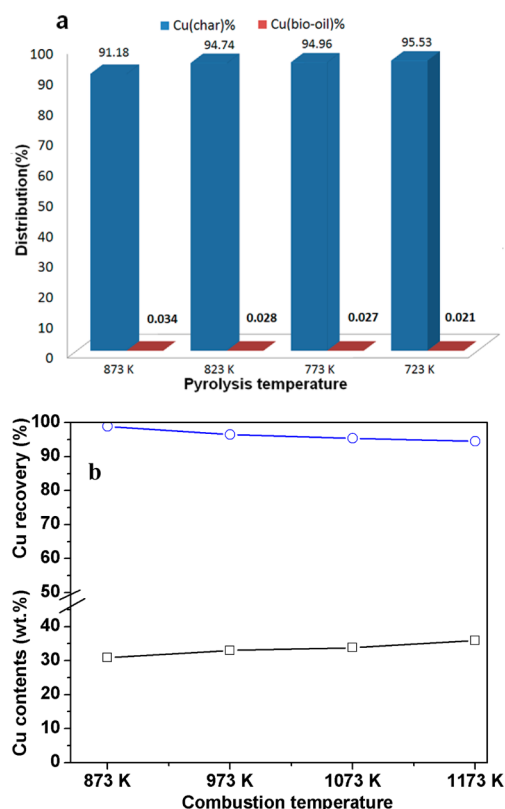
oil. The C11+ compounds, the incompletely chain-breaking decomposed products of lignin, accounted for only a small proportion in the bio-oils. The results above reveal that the presence of Cu could effectively catalyze the chain-breaking decomposition of lignin to produce more C7−C10 compounds. The results of GC-MS are consistent with those of UV-vis and ^{1}H NMR spectra, suggesting that the Cu present in biomass can catalyze the thermal decomposition of lignin structure to small-molecular aromatic compounds.

Figure 5. (a) Distribution of Cu in the char and the bio-oil produced at different pyrolysis temperatures with an initial Cu content of Cu-FSD of 1.09 wt %; and (b) the Cu contents of the ash and Cu recovery after combusted at different temperatures (Cu content of biochar here was 3.54 wt.%, and Cu recovery was calculated as follows: Cu reccovery % = ((Cu content of the ash × amount of the ash after combustion)/(Cu content of the bio-char × amount of the bio-char before combustion)) × 100%.
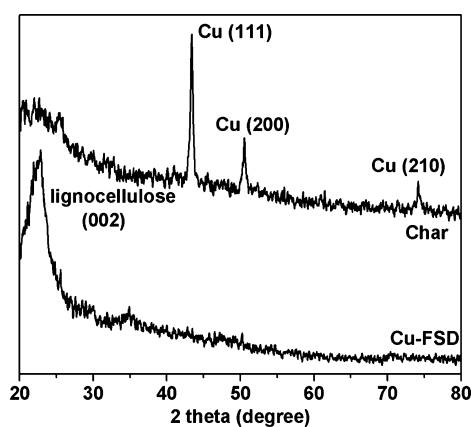

Figure 6. XRD patterns of the Cu-FSD (Cu contents: 1.09 wt %) and its pyrolysis char at 773 K.

The Cu-FSD and its pyrolysis char were characterized by XPS to investigate the oxidation state changes of Cu (Figure 7). The copper in Cu(II) oxidation state gives a shakeup satellite peak at binding energy of about 10 eV higher than that of Cu2p 3/2 excitation, which cannot be observed in Cu(I) and Cu(0) oxidation states. This feature is usually used to distinguish between Cu(II) and the low valence copper, that is, Cu(I) and Cu(0).[48] In the spectrum of Cu-FSD, a satellite peak was observed at binding energy of 943.0 eV, which is 8.8 eV higher
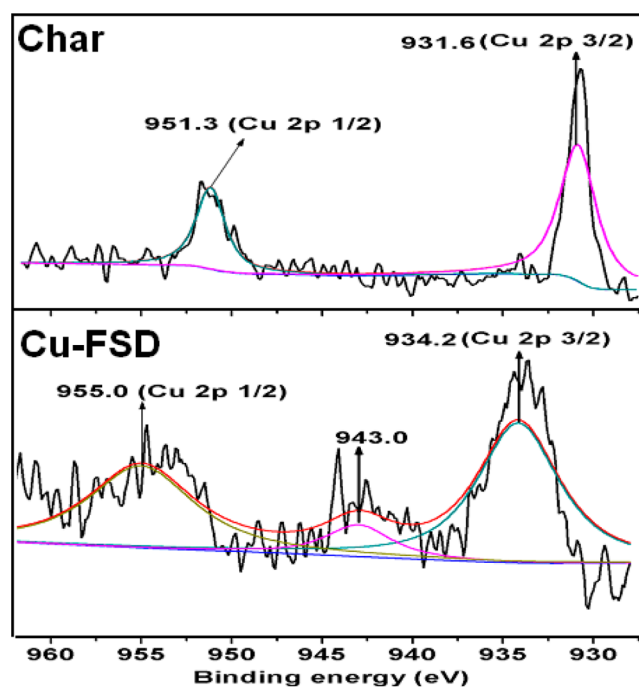

Figure 7. XPS fitting curves of Cu 2p for the Cu-FSD (Cu content: 1.09 wt %) and its pyrolysis char at 773 K.

than that of the Cu2p 3/2 excitation (934.2 eV), and disappeared in the spectrum of the char. Meanwhile, the binding energy of Cu 2p 3/2 excitation decreased to 931.6 eV. These results demonstrate that low valence copper was formed in the pyrolysis process.

The XPS and XRD results, confirm that the copper was in amorphous Cu(II) state in the Cu-FSD, and reduced to face-centered cubic crystal Cu(0) state after pyrolysis. A possible mechanism of the formation of zerovalent Cu (SI Figure S3) is proposed on the basis of the analytical results above. In the pyrolysis process, the covalent bonds in the biomass molecules, for example, C−C and C−O, are broken to produce the radicals, and further form incondensable gas and bio-oil vapor, leaving some free electrons (e−). The in situ generated e− is then captured by Cu(II) to form Cu(0).

Implications. The HMPB is not only generated from heavy metal biosorption process, it can also originate from phytoremediation of metal polluted water body, abandoned mines, and even activated sludge. Fast pyrolysis is an environmentally friendly technology for converting the HMPB into bio-oil, which has a great potential use as fuel or chemicals. In the industrial application of this technology, to make full use of the catalytic effect of Cu, the Cu contents of HMPB can be easily adjusted by varying the biomass amount used in the adsorption process. In the fast pyrolysis of HMPB, more than 91% of the Cu in the HMPB is enriched in the biochar, whereas the Cu content in the bio-oil fraction is very low, ensuring that the bio-oil can find its application in many fields without secondary pollution of heavy metals. The Cu-enriched biochar can be reused to supply heat for the fast pyrolysis. After burning, the Cu contents of the ash are more 30 wt.%, and no significant volatilization of Cu is found in the combustion process. In summary, the approach demonstrated in this work opens up a new way to comprehensively use the waste biomass.

■ ASSOCIATED CONTENT

S **Supporting Information**

Additional descriptions about the experiments (S1); Tables S1–S4; and Figures S1–S4 are provided in SI. This material is available free of charge via the Internet at http://pubs.acs.org.

■ AUTHOR INFORMATION

Corresponding Author
*Fax: +86-551-3607482; e-mail: jhong@ustc.edu.cn.

Notes

The authors declare no competing financial interest.

■ ACKNOWLEDGMENTS

■ REFERENCES

(1) Qiu, J. China faces up to groundwater crisis. *Nature* **2010**, *466*, 308–308.

(2) Godfray, H. C. J.; Beddington, J. R.; Crute, I. R.; Haddad, L.; Lawrence, D.; Muir, J. F.; Pretty, J.; Robinson, S.; Thomas, S. M.; Toulmin, C. Food security: The challenge of feeding 9 billion people. *Science* **2010**, *327*, 812–818.

(3) Schwarzenbach, R.; Escher, P. B.; Fenner, I. K.; Hofstetter, T. B.; Johnson, C. A.; Gunten, U.; Wehrli, B. The challenge of micropollutants in aquatic systems. *Science* **2006**, *313*, 1072–1077.

(4) Nriagu, J. O.; Pacyna, J. M. Quantitative assessment of worldwide contamination of air, water and soils by trace metals. *Nature* **1988**, *333*, 134–139.

(5) Liu, J. F.; Zhao, Z. S.; Jiang, G. B. Coating Fe_3O_4 magnetic nanoparticles with humic acid for high efficient removal of heavy metals in water. *Environ. Sci. Technol.* **2008**, *42*, 6949–6954.

(6) Luo, T.; Cui, J.; Hu, S.; Huang, Y.; Jing, C. Arsenic removal and recovery from copper smelting wastewater using TiO_2. *Environ. Sci. Technol.* **2010**, *44*, 9094–9098.

(7) Shannon, M. A.; Bohn, P. A.; Elimelech, M.; Georgiadis, J. G.; Marinas, B. J.; Mayes, A. M. Science and technology for water purification in the coming decades. *Nature* **2008**, *452*, 301–310.

(8) Agunbiade, O. F.; Olu-Owolabi, B. I.; Adebowale, K. O. Phytoremediation potential of *Eichornia crassipes* in metal-contaminated coastal water. *Bioresour. Technol.* **2009**, *100*, 4521–4526.

(9) Salt, D. E.; Blaylock, M.; Kumar, N. P. B. A.; Dushenkov, V.; Ensley, B. D.; Chet, I.; Raskin, I. Phytoremediation: A novel strategy for the removal of toxic metals from the environment using plants. *Nat. Biotechnol.* **1995**, *13*, 468–474.

(10) Hsu, L. C.; Wang, S. L.; Lin, Y. C.; Wang, M. K.; Chiang, P. N.; Liu, J. C.; Kuan, W. H.; Chen, C. C.; Tzou, Y. M. Cr(VI) removal on fungal biomass of *neurospora crassa*: The importance of dissolved organic carbons derived from the biomass to Cr(VI) reduction. *Environ. Sci. Technol.* **2010**, *44*, 6202–6208.

(11) Wang, J.; Chen, C. Biosorbents for heavy metals removal and their future. *Biotechnol. Adv.* **2009**, *27*, 195–226.

(12) Park, D.; Yun, Y.-S.; Jo, J. H.; Park, J. M. Biosorption process for treatment of electroplating wastewater containing Cr(VI): Laboratory-scale feasibility test. *Ind. Eng. Chem. Res.* **2006**, *45*, 5059–5065.

(13) Yu, J.; Tong, M.; Sun, X.; Li, B. Enhanced and selective adsorption of Pb^{2+} and Cu^{2+} by EDTAD-modified biomass of baker's yeast. *Bioresour. Technol.* **2008**, *99*, 2588–2593.

(14) Czernik, S.; Bridgwater, A. V. Overview of applications of biomass fast pyrolysis oil. *Energy Fuels* **2004**, *18*, 590–598.

(15) Huber, G. W.; Iborra, S.; Corma, A. Synthesis of transportation fuels from biomass: Chemistry, catalysts, and engineering. *Chem. Rev.* **2006**, *106*, 4044–4098.

(16) Vispute, T. P.; Zhang, H. Y.; Sanna, A.; Xiao, R.; Huber, G. W. Renewable chemical commodity feedstocks from integrated catalytic processing of pyrolysis oils. *Science* **2010**, *330*, 1222–1227.

(17) Shen, G.; Tao, S.; Wang, W.; Yang, Y.; Ding, J.; Xue, M.; Min, Y.; Zhu, C.; Shen, H.; Li, W.; Wang, B.; Wang, R.; Wang, W.; Wang, X.; Russell, A. G. Emission of oxygenated polycyclic aromatic hydrocarbons from indoor solid fuel combustion. *Environ. Sci. Technol.* **2011**, *45*, 3459–3465.

(18) Liu, W.-J.; Zeng, F.-X.; Jiang, H.; Zhang, X.-S.; Yu, H.-Q. Techno-economic evaluation of the integrated biosorption-pyrolysis technology for lead (Pb) recovery from aqueous solution. *Bioresour. Technol.* **2011**, *102*, 6260–6265.

(19) Ryden, M.; Johansson, M.; Lyngfelt, A.; Mattisson, T. NiO supported on $Mg–ZrO_2$ as oxygen carrier for chemical-looping combustion and chemical-looping reforming. *Energy Environ. Sci.* **2009**, *2*, 970–981.

(20) Matsumura, Y.; Ishibe, H. High temperature steam reforming of methanol over $Cu/ZnO/ZrO_2$ catalysts. *Appl. Catal. B: Environ.* **2009**, *91*, 524–532.

(21) Larsen, A. O.; Leu, W.; Oberhuber, C. N.; Campbell, J. E.; Hoveyda, A. H. Bidentate NHC-based chiral ligands for efficient Cu-catalyzed enantioselective allylic alkylations: Structure and activity of an air-stable chiral Cu complex. *J. Am. Chem. Soc.* **2004**, *126*, 11130–11131.

(22) Lin, K. S.; Wang, H. P. Supercritical water oxidation of 2-chlorophenol catalyzed by Cu^{2+} cations and copper oxide clusters. *Environ. Sci. Technol.* **2000**, *34*, 4849–4854.

(23) Fan, Y.; Lu, X.; Ni, Y.; Zhang, H.; Zhao, L.; Chen, J.; Sun, C. Destruction of polychlorinated aromatic compounds by spinel-type complex oxides. *Environ. Sci. Technol.* **2010**, *44*, 3079–3084.

(24) Huang, J.; Cui, Y.; Wang, X. Visible light-sensitive ZnGe oxynitride catalysts for the decomposition of organic pollutants in water. *Environ. Sci. Technol.* **2010**, *44*, 3500–3504.

(25) Lin, Y.-C.; Huber, G. W. The critical role of heterogeneous catalysis in lignocellulosic biomass conversion. *Energy Environ. Sci.* **2009**, *2*, 68–80.

(26) Zheng, M. Y.; Wang, A. Q.; Ji, N.; Pang, J. F.; Wang, X. D.; Zhang, T. Transition metal–tungsten bimetallic catalysts for the conversion of cellulose into ethylene glycol. *ChemSusChem* **2010**, *3*, 63–66.

(27) Kunkes, E. L.; Simonetti, D. A.; West, R. M.; Serrano-Ruiz, J. C.; Gärtner, C. A.; Dumesic, J. A. Catalytic conversion of biomass to monofunctional hydrocarbons and targeted liquid-fuel classes. *Science* **2008**, *322*, 417–421.

(28) Fan, Y.; Xiao, H.; Shi, G.; Liu, H.; Bao, X. A novel approach for modulating the morphology of supported metal nanoparticles in hydrodesulfurization catalysts. *Energy Environ. Sci.* **2011**, *4*, 572–582.

(29) Chang, S. H.; Yeh, J. W.; Chein, H. M.; Hsu, L. Y.; Chi, K. H.; Chang, M. B. PCDD/F adsorption and destruction in the flue aas streams of MWI and MSP via Cu and Fe catalysts supported on carbon. *Environ. Sci. Technol.* **2008**, *42*, 5727–5733.

(30) Landong, L.; Jixin, C.; Shujuan, Z.; Fuxiang, Z.; Naijia, G.; Tianyou, W.; Shuliang, L. Selective catalytic reduction of nitrogen oxides from exhaust of lean burn engine over in-situ synthesized Cu–ZSM-5/cordierite. *Environ. Sci. Technol.* **2005**, *39*, 2841–2847.

(31) Liu, W. J.; Zeng, F. X.; Jiang, H.; Yu, H. Q. Total recovery of nitrogen and phosphorus from three wetland plants by fast pyrolysis technology. *Bioresour. Technol.* **2011**, *102*, 3471–3479.

(32) Cho, J.; Davis, J. M.; Huber, G. W. The intrinsic kinetics and heats of reactions for cellulose pyrolysis and char formation. *ChemSusChem* **2010**, *3*, 1162–1165.

(33) DeSisto, W. J.; Hill, N.; Beis, S. H.; Mukkamala, S.; Joseph, J.; Baker, C.; Ong, T.-H.; Stemmler, E. A.; Wheeler, M. C.; Frederick, B. G.; van Heiningen, A. Fast pyrolysis of pine sawdust in a fluidized-bed reactor. *Energy Fuels* **2010**, *24*, 2642–2651.

(34) Westerhof, R. J. M.; Brilman, D. W. F.; van Swaaij, W. P. M.; Kersten, S. R. A. Effect of temperature in fluidized bed fast pyrolysis of biomass: Oil quality assessment in test units. *Ind. Eng. Chem. Res.* **2009**, *49*, 1160–1168.

(35) Wang, P.; Zhan, S. H.; Yu, H. B.; Xue, X. F.; Hong, N. The effects of temperature and catalysts on the pyrolysis of industrial wastes (herb residue). *Bioresour. Technol.* **2010**, *101*, 3236−3241.

(36) Hoekstra, E.; Westerhof, R. J. M.; Brilman, W.; Van Swaaij, W. P. M.; Kersten, S. R. A.; Hogendoorn, K. J. A.; Windt, M. Heterogeneous and homogeneous reactions of pyrolysis vapors from pine wood. *AIChE J.* **2012**, DOI: 10.1002/aic.12799.

(37) Friedl, A.; Padouvas, E.; Rotter, H.; Varmuza, K. Prediction of heating values of biomass fuel from elemental composition. *Anal. Chim. Acta* **2005**, *544*, 191−198.

(38) Zakzeski, J.; Bruijnincx, P. C. A.; Jongerius, A. L.; Weckhuysen, B. M. The catalytic valorization of lignin for the production of renewable chemicals. *Chem. Rev.* **2010**, *110*, 3552−3599.

(39) Skutil, K.; Czechowicz, D.; Taniewski, M. Nitrogen-rich natural gases as a potential direct feedstock for some novel methane transformation processes. Part 2: Non-oxidative processes. *Energy Fuels* **2009**, *23*, 4449−4459.

(40) Zhang, H.; Xiao, R.; Wang, D.; Zhong, Z.; Song, M.; Pan, Q.; He, G. Catalytic fast pyrolysis of biomass in a fluidized bed with fresh and spent fluidized catalytic cracking (FCC) catalysts. *Energy Fuels* **2009**, *23*, 6199−6206.

(41) Singh, S. K.; Srinivasa, R. M.; Mangle, M.; Ravi Ganesh, K. Cu(I)-mediated deoxygenation of N-oxides to amines. *Tetrahedron* **2007**, *63*, 126−130.

(42) Dean, J. A. *Lange's Hand Book of Chemistry*, 15th ed.; McGraw-Hill Book Company: New York, 1999.

(43) Amen-Chen, C.; Pakdel, H.; Roy, C. Production of monomeric phenols by thermochemical conversion of biomass: A review. *Bioresour. Technol.* **2001**, *79*, 277−299.

(44) Tsai, W. T.; Lee, M. K.; Chang, Y. M. Fast pyrolysis of rice husk: Product yields and compositions. *Bioresour. Technol.* **2007**, *98*, 22−28.

(45) Azeez, A. M.; Meier, D.; Odermatt, J. R.; Willner, T. Fast pyrolysis of African and European lignocellulosic biomasses using Py-GC/MS and fluidized bed reactor. *Energy Fuels* **2010**, *24*, 2078−2085.

(46) Stals, M.; Thijssen, E.; Vangronsveld, J.; Carleer, R.; Schreurs, S.; Yperman, J. Flash pyrolysis of heavy metal contaminated biomass from phytoremediation: Influence of temperature, entrained flow and wood/leaves blended pyrolysis on the behaviour of heavy metals. *J. Anal. Appl. Pyrolysis* **2010**, *87*, 1−7.

(47) Shen, D. K.; Gu, S. The mechanism for thermal decomposition of cellulose and its main products. *Bioresour. Technol.* **2009**, *100*, 6496−6504.

(48) Arena, F.; Barbera, K.; Italiano, G.; Bonura, G.; Spadaro, L.; Frusteri, F. Synthesis, characterization and activity pattern of Cu-ZnO/ZrO$_2$ catalysts in the hydrogenation of carbon dioxide to methanol. *J. Catal.* **2007**, *249*, 185−194.